Optical nonlinearity of nanocrystalline Au/ZnO composite films

Hongbo Liao

Department of Physics, Hong Kong University of Science and Technology, Clear Water Bay, Kowloon, Hong Kong, China, and Department of Physics, Beijing Normal University, Beijing 100875, China

Weijia Wen and George K. L. Wong

Department of Physics and Institute of Nano Science and Technology, Hong Kong University of Science and Technology, Clear Water Bay, Kowloon, Hong Kong, China

Guozhen Yang

Institute of Physics, Chinese Academy of Science, Beijing 100080, China

Received January 29, 2003

The third-order nonlinear optical susceptibilities, $\chi^{(3)}$, of composite films consisting of nanocrystalline Au and ZnO particles were investigated by use of a degenerate four-wave mixing scheme. The maximum value of $\chi^{(3)}$, measured at a laser wavelength of 532 nm and a pulse duration of 70 ps, was $\sim 2 \times 10^{-6}$esu. Also, this $\chi^{(3)}$ value was achieved with small absorption (the surface-plasmon peak was at the 615-nm wavelength). Our composite materials showed no discernible degradation after they were subjected to irradiation for a total of 3×10^{7} high-intensity pulses (24 Mw/cm^2, 70-ps pulse duration at 500 Hz) during 16 h of testing. © 2003 Optical Society of America

OCIS codes: 160.4330, 190.4380, 320.5390, 360.6550.

Materials with large third-order nonlinear susceptibility, $\chi^{(3)}$, are essential for future optical device applications.[1,2] Composite consisting of metal nanoparticles (Au, Ag, or Cu) embedded in a dielectric matrix attracted much attention recently because of their fast response time and large $\chi^{(3)}$, which stem from large local field enhancement near the surface-plasmon resonance (SPR).[3,4] Several kinds of dielectric materials have been used as the matrices to further improve the nonlinearity of metal composites,[5–8] but the contributions from the matrices to the nonlinear enhancement of the composites have usually been neglected because of the composites' much smaller $\chi^{(3)}$ compared with that of metal particles. Semiconductor quantum dots are another kind of nonlinear material with a large value of $\chi^{(3)}$ as a result of the quantum confinement effect.[3] A common drawback to these two kinds of composites is the close association of the large $\chi^{(3)}$ with resonance absorption, which may cause thermal damage. For practical application, nonlinear materials with a large off-resonant value of $\chi^{(3)}$ are very important. In this Letter we report an investigation of the nonlinearity of composite films consisting of nanocrystalline Au and ZnO particles. This type of nonlinear thin-film material may be practical for applications in nonlinear optical devices in the future.

Au/ZnO composite films were prepared in a multitarget magnetron sputtering system, described in detail elsewhere.[5] A Au (99.999%) target and a Zn (99.999%) target were connected to two independent rf power supplies, and they were alternately deposited onto a fused quartz substrate at room temperature. We introduced oxygen into the deposition system to form ZnO films. When the pressure ratio of Ar:O$_2$ was set at 8:2, the growth rates of Au and ZnO were approximately 0.1 and 0.04 nm/s with sputtering power of the Au and Zn targets of 25 and 80 W, respectively. The refractive index of the pure ZnO films that were obtained was measured to be 1.9 (at the wavelength of 632.8 nm), very close to that of ZnO crystals (~2.01).[9] The thickness of the Au layer was ~3 nm. After deposition, the Au/ZnO films were annealed in a program-controlled thermal furnace for 2 h at a temperature ranging from 300 to 1050 °C. All the Au/ZnO films used in this Letter, either before or after thermal annealing, were of the same Au concentration, ~20% in atomic fraction as measured by x-ray fluorescence spectroscopy.

The powder x-ray diffraction (XRD) method was applied to characterize the structure of the composite films (Fig. 1). There is no diffraction peak for either Au or ZnO in the as-grown film (curve A of Fig. 1). This indicates that both components were either amorphous or consisted of very small particles. After annealing for 2 h at a temperature below 950 °C, both components crystallized, and diffraction peaks emerged (curves B–D). It is obvious that the ZnO particles may have a textured structure along the ⟨001⟩ direction. However, with increasing annealing time (curve E) and temperature (curve F), the ZnO (001) peak gradually disappeared and a new phase, Zn$_2$SiO$_4$, formed as a result of the chemical reaction between ZnO and the quartz substrate.

To investigate the microstructure, we employed transmission electron microscopy to image the cross section of the Au/ZnO films. Selected pictures are shown in Fig. 2. It can be seen that the as-deposited film has a layer-by-layer structure with a period of

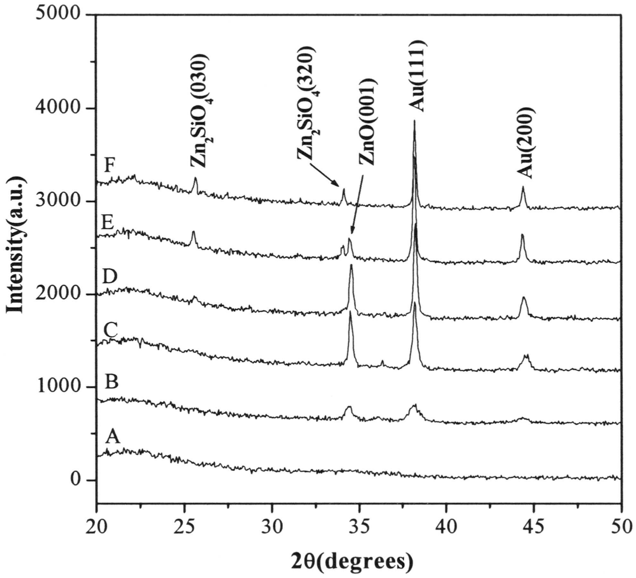

Fig. 1. XRD pattern for Au/ZnO composite films. A, the as-deposited film; the other films are annealed at B, 450 °C for 2 h; C, 750 °C for 2 h; D, 950 °C for 2 h; E, 950 °C for 10 h; and F, 1050 °C for 2 h.

~10 nm, whereas the Au particles are very small (20–70 nm in diameter) and nearly connected to form semicontinuous layers (see the white lines in Fig. 2A). The microstructure can be seen to vary significantly after thermal annealing (Figs. 2B and 2C). Even when the film was annealed at a temperature as low as 300 °C, small particles of crystalline Au and ZnO began to form (Fig. 2B). When the annealing temperature was increased to 750 °C, two things occurred. First, ZnO from different layers joined together to form ZnO crystallites, as indicated in Fig. 2C. Second, Au diffused to the top and the bottom of the film to form larger particles, leaving only some smaller Au particles embedded inside and thus resulting in a wide size distribution of Au particles. In this case, the interface between the film and the quartz substrate was still clearly delineated (by the unlabeled arrow). However, when the annealing temperature was further increased to 1050 °C (Fig. 2D), the interface became rough and the Au particles could be found only at the top surface. A new Zn_2SiO_4 layer (this composition was confirmed by XRD; see curve F of Fig. 1) was formed between the film and the quartz substrate.

Optical absorption spectra were measured by an ultraviolet–visible spectrometer (Perkin Elmer, Lambda20) in a wavelength range 300–1000 nm. The results are shown in Fig. 3. The as-deposited film was observed to have a light brown color and had no SPR peak in the visible range (curve A). After annealing at 300 °C for 2 h, the film color changed to purple, with a SPR peak located at 581 nm (curve B). When the annealing temperature increased to 600–750 °C, the film appeared a beautiful blue and the SPR peak redshifted to near 615 nm (curves C and D) because of the increase in the size of Au particles. This SPR peak was very close to that estimated from Mie theory by use of the dielectric spectra of Au particles. On the other hand, the SPR peak of Au:ZnO was subjected to a redshift and broadening compared with that of Au:SiO_2 composite (located at ~530 nm),[5] because the Au:ZnO composite had a matrix material (ZnO) with a larger refractive index and a wide size distribution. Further increasing the annealing temperature to 950 °C was seen to shift the SPR peak back to 592 nm; this shift was accompanied by a decrease in the optical density (curve E) as a result of light scattering and further broadening of the SPR peak caused by the very large Au particles (larger than 100 nm in diameter). It should be noted that the small but narrow absorption peak near 365 nm arose from the exciton absorption of ZnO nanocrystallites. This peak disappeared in the

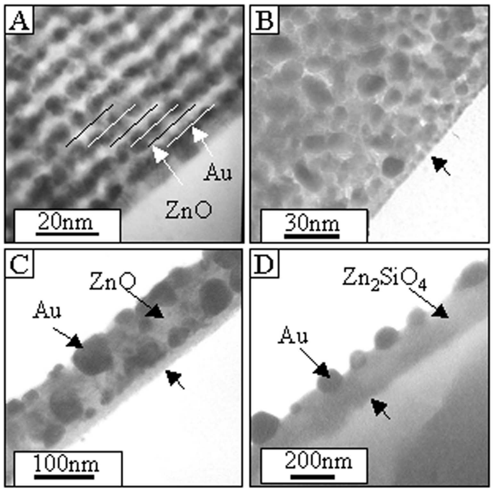

Fig. 2. Selected cross-sectional transmission electron microscopy pictures of the Au/ZnO films at various stages of annealing: A, as-deposited film; B, annealing at 300 °C for 2 h; C, annealing at 750 °C for 2 h; and D, annealing at 1050 °C for 2 h.

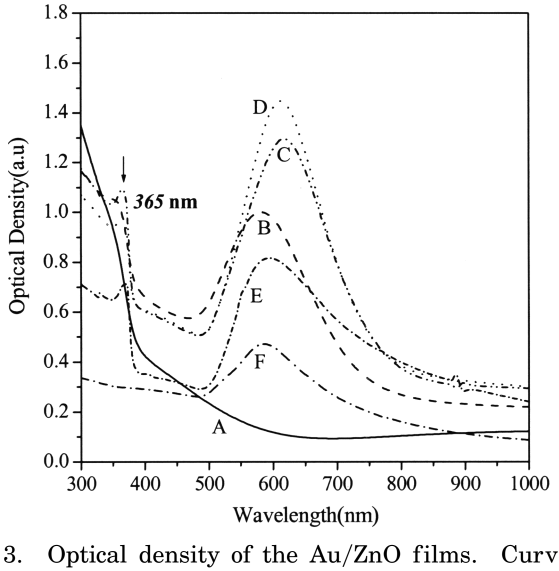

Fig. 3. Optical density of the Au/ZnO films. Curve A, as-deposited film; curves B, C, D, E, and F, films annealed for 2 h at 300, 600, 750, 950, and 1050 °C.

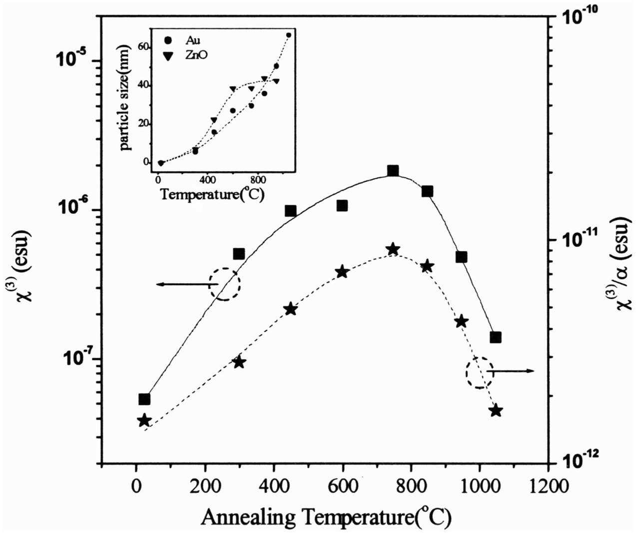

Fig. 4. Co-plot of measured $\chi^{(3)}$ and FOM versus annealing temperature. The squares represent $\chi^{(3)}$, while the stars denote FOM. The solid and dashed curves are to guide the eye. Inset, relationship between the annealing temperature and the particle sizes of Au (circles) and ZnO (triangles).

film after annealing at 1050 °C (curve F of Fig. 3), at the formation of Zn_2SiO_4 (see curve F of Fig. 1).

The third-order nonlinear susceptibility, $\chi^{(3)}$, was measured at 532 nm by use of a Q-switched and mode-locked Nd:YAG laser with a pulse duration of 70 ps, a maximum peak power of ~24 MW cm^{-2} (the beam spot was ~0.5 mm), and a standard backward degenerate four-wave mixing scheme. Because of the smaller optical absorption at 532 nm, our Au/ZnO films can be subjected to much more intense laser radiation than Au/SiO_2, without suffering any discernible degradation in their optical properties. The value of the effective $\chi^{(3)}$ was measured relative to that of a reference, CS_2, taken to be 2×10^{-12} esu in the picosecond regime.[10] During the measurement of nonlinearity, we noticed that the background of the signal coming mainly from the light scattering of the Au:ZnO composite was very small. This small signal background indicates that our samples can be regarded as a uniform system, although they had an inhomogeneous microstructure.

The measured $\chi^{(3)}$ and the figure of merit (FOM), $\chi^{(3)}/\alpha$, are co-plotted versus annealing temperature in Fig. 4. The as-deposited film (at 25 °C) has very small $\chi^{(3)}$ ($\sim 5 \times 10^{-8}$ esu) and FOM ($\sim 1.5 \times 10^{-12}$ esu). With increasing annealing temperature, both $\chi^{(3)}$ and FOM increase to a maximum value at 750 °C. The maximum values [$\chi^{(3)} \sim 1.8 \times 10^{-6}$ esu; FOM, $\sim 9 \times 10^{-12}$ esu] of Au/ZnO films are comparable to those of Au/SiO_2 films measured at their SPR with the same laser.[5] This implies that the Au/ZnO films have a much larger resonant third-order nonlinearity, because, first, $\chi^{(3)}$ of ZnO is two orders of magnitude larger than that of SiO_2,[10] and, second, the larger dielectric constant of ZnO results in a larger local field factor, which may influence the enhancement of $\chi^{(3)}$ following a power law. However, with a further increase in the annealing temperature, the values of $\chi^{(3)}$ and FOM were seen to decrease sharply.

The inset of Fig. 4 shows the relationship between the Au and ZnO particle sizes and the annealing temperature. Here the particle size was acquired from the XRD peak by use of the Scherrer equation. It can be seen that the Au particle size increased monotonically with increasing annealing temperature, whereas the ZnO particles first grew rapidly with increasing annealing temperature but then remained at ~40 nm for annealing temperatures higher than 650 °C. Thus the Au/ZnO film has a maximum $\chi^{(3)}$ value at an average Au particle size of ~30 nm, very close to the skin depth of bulk metal Au in the visible range.[11] It is proposed that the relationship between the nonlinearity and the annealing temperature is due to this Au particle size variation. Further improvement in the value of $\chi^{(3)}$ may thus be achieved by narrowing of the particle size distribution to peak at the optimal size.

This work was supported by the Research Grants Council (RGC) of Hong Kong through grant HKUST 6153/00P and Natural Science Foundation of China (NSFC)–RGC co-project N_HKUST 025/00. We thank P. Sheng for helpful discussions. W. Wen's e-mail address is phwen@ust.hk.

References

1. Y. R. Shen, *The Principles of Nonlinear Optics* (Wiley, New York, 1984).
2. J. I. Sakai, *Phase Conjugate Optics* (McGraw-Hill, New York, 1994).
3. C. Flytzanis, F. Hache, M. C. Klein, D. Ricard, and P. Rousignol, *Progress in Optics XXIX* E. Wolf, ed. (North-Holland, Amsterdam, 1991).
4. D. Ricard, P. Roussignol, and C. Flytzanis, Opt. Lett. **10,** 511 (1985).
5. H. B. Liao, R. F. Xiao, J. S. Fu, H. Wang, K. S. Wong, and G. K. L. Wong, Opt. Lett. **23,** 388 (1998).
6. J. M. Ballesteros, R. Serna, J. Solis, C. N. Afonos, A. K. Petford-Long, D. M. Osborne, and R. F. Haglund, Jr., Appl. Phys. Lett. **71,** 2445 (1997).
7. G. Yang, W. Wang, Y. Zhou, Y. Lu, G. Yang, and Z. Chen, Appl. Phys. Lett. **81,** 3969 (2002).
8. S. Ogawa, Y. Hayashi, N. Kobayashi, T. Tokizaki, and A. Nakamura, Jpn. J. Appl. Phys. **33,** L331 (1994).
9. M. J. Weber, ed., *Handbook of Laser Science and Technology* (CRC, Boca Raton, Fla., 1995), Suppl. 2: Optical Material.
10. R. L. Sutherland, *Handbook of Nonlinear Optics* (Marcel Dekker, New York, 1996).
11. U. Kreibig and M. Vollmer, *Optical Properties of Metal Clusters* (Springer-Verlag, Berlin, 1995).